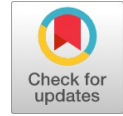


# Deep Learning Approach for Advanced COVID-19 Analysis



Rania Alhalaseh, Mohammad Abbadi, Sura Kassarbeh

**Abstract:** Since the spread of the COVID-19 pandemic, the number of patients has increased dramatically, making it difficult for medical staff, including doctors, to cover hospitals and monitor patients. Therefore, this work depends on Computerized Tomography (CT) scan images to diagnose COVID-19. CT scan images are used to diagnose and determine the severity of the disease. On the other hand, Deep Learning (DL) is widely used in medical research, making great progress in medical technologies. For the diagnosis process, the Convolutional Neural Network (CNN) algorithm is used as a type of DL algorithm. Hence, this work focuses on detecting COVID-19 from CT scan images and determining the severity of the illness. The proposed model is as follows: first, classifying CT scan images into infected or not infected using one of the CNN structures, Residual Neural Networks (ResNet50); second, applying a segmentation process for the infected images to identify lungs and pneumonia using the SegNet algorithm (a CNN architecture for semantic pixel-wise segmentation) so that the disease's severity can be determined; finally, applying linear regression to predict the disease's severity for any new image. The proposed approach reached an accuracy of 95.7% in the classification process and lung and pneumonia segmentation of 98.6% and 96.2%, respectively. Furthermore, a regression process reached an accuracy of 98.29%.

**Keywords:** Convolutional Neural Network (CNN), Deep Learning, Severity, Segnet, ResNet50, CT scan, VGG16.

## I. INTRODUCTION

In January 2020, the coronavirus (COVID-19) pandemic started; since then, it has spread globally, causing millions of deaths, with huge health implications for human lives. At the time of writing this paper, there were more than 768 million confirmed cases and more than 694 million deaths worldwide. Another measure found 388 million confirmed cases and 571 million deaths globally [1], [2]. There are several common symptoms of COVID-19, such as coughing, fever, dyspnea, musculoskeletal symptoms (myalgia, joint pain, fatigue), and gastrointestinal symptoms [3]. The attention given to COVID-19 has lowered recently, along with the restrictions and fear, but it is still responsible for a high percentage of death rates worldwide [1].

Manuscript received on 28 August 2023 | Revised Manuscript received on 05 September 2023 | Manuscript Accepted on 15 September 2023 | Manuscript published on 30 September 2023.

\*Correspondence Author(s)

**Rania Alhalaseh\***, Department of Data Science, University of Mutah, Karak, Jordan. E-mail: [halaseh@mutah.edu.jo](mailto:halaseh@mutah.edu.jo), ORCID ID: [0009-0000-1145-6001](https://orcid.org/0009-0000-1145-6001)

**Mohammad Abbadi**, Department of Computer Science, University of Mutah, Karak, Jordan. E-mail: [abbadi@mutah.edu.jo](mailto:abbadi@mutah.edu.jo), ORCID ID: [0000-0003-1601-627X](https://orcid.org/0000-0003-1601-627X)

**Sura Kassarbeh**, Department of Computer Science, University of Mutah, Karak, Jordan. E-mail: [soosraoof@gmail.com](mailto:soosraoof@gmail.com), ORCID ID: [0009-0006-2711-2872](https://orcid.org/0009-0006-2711-2872)

© The Authors. Published by Blue Eyes Intelligence Engineering and Sciences Publication (BEIESP). This is an open access article under the CC-BY-NC-ND license <http://creativecommons.org/licenses/by-nc-nd/4.0/>

Disease diagnosis is critical to epidemic management because it provides critical information on minor outbreaks that should be stopped before they spread. The disease is detected through several medical tests. The standard diagnostic technique is Reverse Transcription--Polymerase Chain Reaction (RT-PCR) for respiratory diseases, which states whether the patient is infected or not. However, it is not accurate enough: the follow-up CT chest scan shows the patient is infected [4]. RT-PCR with DNA sequencing is considered the most important and widely used. Nevertheless, other tests are based on reported IgM/IgG antibodies [5].

Recently, applications of Artificial Intelligence (AI) and Deep Learning (DL) algorithms have been widely integrated and used to detect different diseases and help doctors to better investigate them, especially in medical image processing. Specifically, DL has achieved high performance results in disease classification, such as diabetes, attention deficit hyperactivity disorder (ADHD), and many others [6]. Therefore, radiologists and doctors can detect COVID-19 by checking the extracted data from the resulting X-rays images, which forms a good source to create a model based on AI to detect COVID-19 [7].

Deep Learning algorithms use different types of neural networks to perform a given task. There are many types of DL algorithms, such as Convolutional Neural Networks (CNNs), Long Short-Term Memory Networks (LSTMs), and Recurrent Neural Networks (RNNs). CNN is the most used one, and it enables computational models consisting of multiple layers to learn data and make decisions [8].

Along with the rapid development of computer technology, digital image-processing technology was applied widely in the medical field, including subsequent medical diagnosis via organ segmentation and image enhancement and repair. Deep CNNs were utilized to detect pulmonary perivisceral nodules, where CT images are typically divided into several small 2D/3D patches and classified into several pre-defined categories [9].

Technologies provided to treat disease are essential, including decision making to deal with the design of medical facilities. Public health policymakers need the accurate judgment of confirmed cases in the future as ML and DL algorithms take past data and use them to make predictions of the confirmed cases of COVID-19 numbers [10]. An AI-based global diagnostic index has increased diagnostic accuracy for therapeutic purposes [11], ML algorithms are used to analyze clinical data about patients to make a diagnosis [12].

CT scans detect inflammation and fluid in the lungs through imaging diagnostics.



These can lead to shortness of breath and other complications such as lack of oxygen in the blood and the disruption of some body functions. It may be challenging to determine the extent of damage from the disease just by looking at the pictures and diagnosing them [13]. Therefore, this work proposes a model to detect COVID-19 by using DL algorithms to monitor the size of the inflammation and determine its location based on several characteristics, such as the percentage of white in the image, the extent of its spread, and the extent of inflammation in the lung.

The main objective of this work is to a CNN-based diagnostics model to detect COVID-19 from a CT scan of lung images as follows:

- A classification process to determine the status of the patient -infected or not infected- based on CT scan images.
- A segmentation process to determine the location of inflammation in the lungs in order to specify the severity of the disease,
- The use of linear regression to predict the percentage of severity for any case.

The main objective of this work is to accelerate the diagnosis of COVID-19 pneumonia using DL algorithms. The automation of the process helps to doctors further determine oxygen dose. This paper proposes an approach to COVID-19 severity detection based on CNN and determines the location of inflammation in the lungs.

### A. Deep Learning (DL)

DL has become increasingly popular in research and is used in many applications, including text mining, spam detection, image classification, and the retrieval of multimedia concepts [14]. The tremendous advances in the development of the ability to collect data have led to the constant emergence of innovative studies [15]. Computational models in DL algorithms consist of multiple processing layers to represent data in several abstraction layers. The model is trained to classify data such as images, text, or sounds, characterized by high precision [16]. In this case, DL can identify and classify diseases by analyzing medical images. It can also predict the mechanisms of disease treatment. Since the emergence of COVID-19, several studies and approaches have shown the use of DL to detect COVID-19 as quickly as possible [17]. In DL networks, three types of networks can be used: Recursive Neural Networks (RvNNs), Recurrent Neural Networks (RNNs), and CNNs [18]. This study uses CNNs.

CNNs are widely applied in image-recognition problems. CNN consists of three different layers: a convolutional layer, pooling layer, and a fully connected layer, to perform the process effectively. The feature-extraction process is applied by both convolutional and pooling layers [19]. The convolutional layer is the base layer responsible for determining the pattern of features. In this layer, the image is passed through a filter. The filtering results produce a feature map. Kernels are applied in this layer to extract features in the pattern [16]. The pooling layer is the second layer in the CNN, used to apply corresponding mathematical computation on the feature map to reduce the number of feature maps [20]. Finally, the fully connected layer (FC) is the third layer of the CNN, and it works as a multi-layer perception. It uses a Rectified Linear Unit (ReLU), activation

function, and SoftMax activation function to predict the output image [21]. The CNN algorithm contains more than one architecture, and it is an essential aspect in optimizing its performance. Some of these architectures are as follows [22]:

- A Residual Network (ResNet) is challenging to train; it must be provided by a residual educational framework to train networks that are considerably deeper than those currently in use. A ResNet consists of many layers; each layer has its own number of layers, such as 34, 50, 101, 152, and even 1202. ResNet50 is a well-known network with 49 convolutional layers and one FC [23].
- VGG16 was proposed by [24] as a CNN model. It was built to calculate the effect of the CNN model depth on accuracy in a large-scale image-recognition setup. Its main goal is to perform a comprehensive examination of networks with increasing depth using a stand-alone architecture with small convolution filters that show a significant improvement by pushing the depth into 16 weight layers with 1000 categories [25].

### B. CT Scan Image Processing

Due to early disease detection being critical for patient treatment and isolating infected people to prevent the virus from spreading various research efforts have been provided to create more rapid and less expensive ways to locate the virus. The standard test method, RT-PCR, is efficient in terms of time but limited in availability [26]. CT and X-Ray images of COVID-19 patients provide crucial information about their health. Virus-induced pneumonia has a variety of visual appearances [27]. There are numerous phases to the diagnosis of COVID-19 patients based on images from CT or X-ray. First, the lung images are processed, then CNN is used to extract the features. Finally, the traits are used in a diagnostic classification system [28].

## II. RELATED WORK

Recently, several studies have been proposed to analyze and detect COVID-19 using DL from CT scans, and chest X-ray images.

[19] proposed a new model to detect COVID-19 based on a CNN algorithm using 100 chest X-ray images. Half of the patients had COVID-19, and the other half belongs were healthy. The authors presented five models of CNN, ResNet50, ResNet101, ResNet152, InceptionV3, and Inception-ResNetV2. The results of the classifications either COVID-19, normal (healthy), viral pneumonia, and bacterial pneumonia. The best detection accuracy of the proposed approach was 98%.

Moreover, in [21], a classification system to detect COVID-19 was proposed using multi-level thresholding and an SVM. The system is applied to lung X-ray images, where all images were the same size, 512x512 pixels, and stored in JPEG format. The proposed system achieved 95.76% sensitivity, 99.7% specificity, and 97.48% accuracy.

Several studies are designed to describe the COVID-19 identification process based on CT scans. Before classification, most of these studies used lung segmentation. [29], with the DeepLabv3 model, described pulmonary segmentation. The authors used a multi-specific paradigm of three classes as part of the classification COVID-19, ordinary pneumonia, and normal with a classification accuracy of 92.49% and 98.13%. This paper used 3D ResNet-18.

Similarly, [30] used Dense-Net 121 to create a lung mask for the segment of lungs and then used Dense-Net as the standard and COVID-19 clinical classifications structure and achieved accuracies of 90%, 78.93%, and 89.93%.

[31] used X-ray pictures and segments of the lungs by obtaining a mask of the lungs and then separating the lungs from the X-ray image with a fully connected DenseNet. The authors randomly selected several patches from the segments' ResNet18 for classification in sizes 224 to 224. The authors chose K patches randomly during the prediction process and, with majority voting, the authors were able to predict whether the COVID-19 disease would be present or not. In the test dataset, the authors showed an accuracy of 88.9%.

[32] showed how the lungs' involvement in COVID-19 should be considered serious. Each of the five pulmonary lobes received visual scores of 0 to 5, where 0 represents cases without participation and 5 represents more than 75% involvement. A total CT value between 0 (no participation) and 25 was determined as the lung-participation sum (maximum involvement). The study showed that inferior lobes in COVID-19 patients were more inclined to participate in higher CT scores.

For each lung, [33] used the severity index. The lung score was added to give a final severity. Each lung was assigned a score of 0-4 based on the extent of consolidation involvement. The scores for each lung were added to the final severity score. This study found that findings from chest X-rays often showed in the lower area on both sides of the lung among COVID-19 patients.

[34] provided the model for COVID-19 frontal chest X-ray pneumonia with a model for severity score prediction. The severity of lung infections with COVID-19 (and generally pneumonia) may be utilized to de-escalate or escalate care, as well as the effectiveness of therapy control, particularly in ICUs. The images of a COVID-19 database were utilized for this investigation. Retrospectively, three specialists assessed these pictures in terms of lung participation and the degree of opacity. Moreover, a pre-trained neural network model with huge (non-COVID-19) X-ray datasets will be utilized to build features that are predictive of our goal for COVID-19 images. The findings of this study reveal that a regression model based on a subset of outputs from the pre-workout X-ray chest model predicts the geographic extent score with 1.14 MAE and 0.78 MAE with lung dysfunction. The results showed that the provided model might be utilized to determine the severity of COVID-19 lung infections, particularly in critical care units, for escalation or de-escalation and the tracking of treatment efficacy.

Moreover, [35] developed a new strategy for concurrently identifying diseases and predicting conversion times, considering challenges such as high-dimensional data, short sample sizes, outlier influence, and imbalance classification. To accomplish this, they devised a sparsity-regularization term to conduct feature selection and learn the shared information across two tasks, as well as a new way to account for sample weight and the imbalance classification problem. They included 408 CT scan images. The results reveal that the approach obtains the best classification at 85.91% accuracy and a regression correlation coefficient performance of 0.462. Moreover, the accuracy of the proposed approach is 76.97% percent.

### III. PROPOSED WORK

This work presents an approach based on the Deep Learning CNN architecture to classify COVID-19 patients and predict disease severity using CT lung images. CNN algorithms are significantly improved and are characterized using accurate algorithm classification operations. Moreover, the importance of using the CNN algorithm through its structure eliminates the need for feature extraction. The CNN system is trained using image filters and convolution to build static properties to pass to the next layer. Then, the features in the next layer use multiple filters to produce more diverse features until the final features are produced [22]. The proposed model is divided into three phases:

- Classification process: images are categorized into COVID-19-infected or non-infected using the ResNet50 structure. This output is represented as a CNN model. After the CNN model is generated, the test dataset is used to determine the classification's effectiveness performance.
- Severity detection using the segmentation process: another dataset was used that contains mask-segmentation images. The mark (incision) of the disease percentage is revealed through inflammation segmentation in the lung, where the areas infected with the COVID-19 virus are identified, as these areas are segmented. The lung's segmented area is used to calculate the percentage of lung inflammation. The system is then trained using images of COVID-19 patients, where some arithmetic (subtraction) and logical (XOR) operations are used to determine the size, location, and percentage of inflammation in the lung.
- Predicting severity through regression: each image and its disease severity ratio are stored to prepare these data for the testing stage. All the collected data are trained using a linear regression algorithm to predict the incision of the disease and compare the expected values with the actual values to obtain the lowest error rate to predict the incision of the disease for a new image.

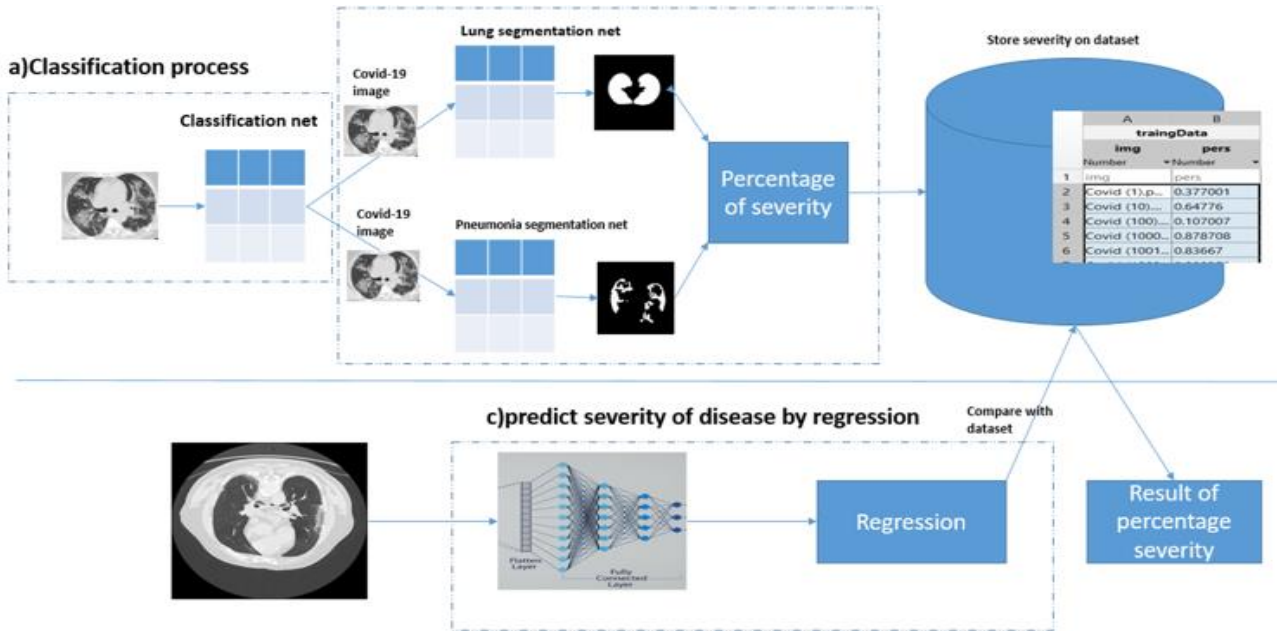


Fig. 1. The Proposed Model

All previous phases are shown in the block diagram in Fig. 1. Furthermore, in the pre-processing stage, the CT images of uninfected and COVID-19 patients are stored in the original dataset and processed to be ready for the training process.

### A. Preprocessing

Image preprocessing refers to the operations that are applied to the images at the basic level of abstraction in order to improve their quality. This is achieved by suppressing unwanted distortions and enhancing some of the image features. This work used these steps: 1) conversion of the medical image to PNG format, 2) image augementer reflection, and 3) histogram equalization.

The images in the dataset are converted into Portable Network Graphics (PNG) format images to be suitable and accepted by DL algorithms. Then, the fixed-size images are used to train neural networks in the training stage. Therefore, all images containing a lung are resized to 224x224 pixels to be appropriate for the network.

Histogram equalization is a technique used in digital image processing, in which the contrast of an image is modified, and its histograms are as flat and distributed as possible [36]. This method usually increases the contrast of many images, especially when data are represented by contrast values that are close to each other. Light intensity values are better distributed over the image histogram during the adjustment process; therefore, the areas with little localized contrast can have more contrast. This technique was applied to dark images, increasing the contrast by detecting the distribution of pixel densities in an image and plotting these pixel densities on a histogram. Fig. 2 shows an example of the application of histogram equalization on one of the images.

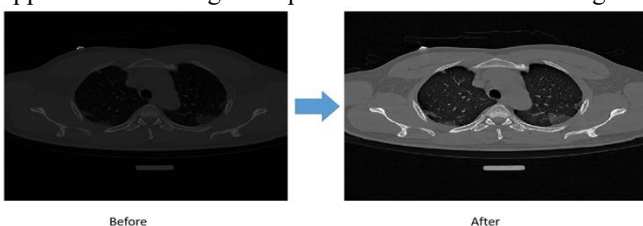


Fig. 2. Histogram Equalization Applied to One of the Images.

### B. CNN Model

The CNN uses filters and image convolution to create static features whereby adjacent pixels are grouped, divided into classes, and then passed to the next layer. Then, the feature is wrapped in the next layer with different filters to obtain more different features to produce the final features. The advantage of the CNN algorithm is that it is not necessary for it to extract features because the CNN architecture extracts feature on its own [8].

- **Input Layer:** in this layer, the images are utilized as input for the CNN in the input layer, representing the images' pixels matrix, as shown in Fig. 3

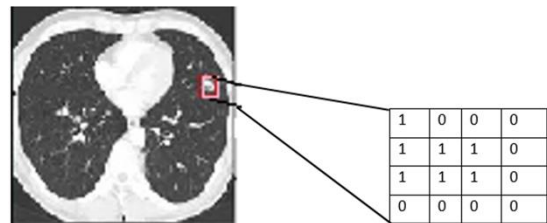


Fig. 3. Input Image Matrix

- **Convolution Layer:** This is the first layer and the most critical component of CNN design. It consists of a set of convolutional filters (so-called kernels). In this layer, the output feature map is created by convolving the input image, represented as an N-dimensional metrics with kernels. For example, a 4x 4 grey-scale image uses a 2x2 random-weight initialized kernel to better understand the convolutional operation. First, the kernel moves horizontally and vertically across the entire image. In addition, the dot product between the input picture and the kernel is calculated. Their respective values are multiplied, and then the sum value of the dot product result is calculated to generate a single scalar value. The whole process is repeated until no further sliding is possible.

Therefore, the calculated dot product values represent the feature map of the output. Fig. 4 illustrates the preliminary calculations executed at each step. In this figure, the light green color represents 2x2 kernels, while the light blue color represents a similar size area of the input image. After calculating the sum value's dot product results (marked in light orange), the sum value represents an input value to the output feature map.

- **Pooling Layer:** The pooling layer subsamples the feature maps. In other words, this method reduces the size of enormous feature maps to create smaller ones. At the same time, it preserves most information (or characteristics) at each stage of the pooling process. Before the pooling process, both the stride and the kernel are size assigned in the same way as the convolutional operation is. Fig. 5 shows three pooling methods. They use the most significant number of each local cluster from the feature maps, the min-pooling uses the lowest value, and the average pooling method uses the average number from the selected region. Flattening is performed after the pooling-layer process to convert all 2D arrays from pooled features into a single, long, continuous vector, as shown in Fig. 6 The output is used as input for the continuous layer.
- **Fully Connected Layer (FC):** The Fully connected layer connects each neuron in this layer to all neurons in the previous layer. This layer receives its input from the previous pooling or convolutional layer. This input is formed as a vector by flattening the feature maps. Then, the output represents the final CNN output. In this phase, the flattened matrices are passed through the FC layer, and then the classification process begins.

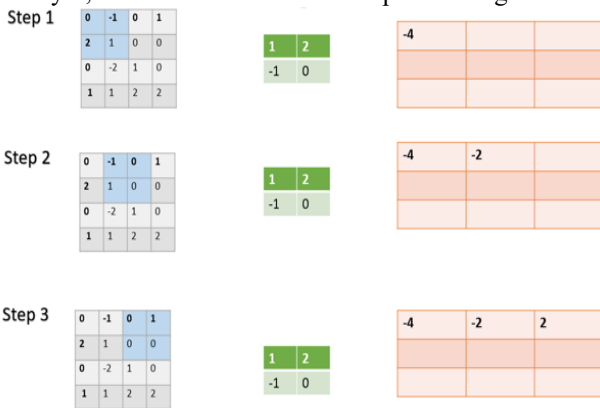


Fig. 4. Convolution Operation

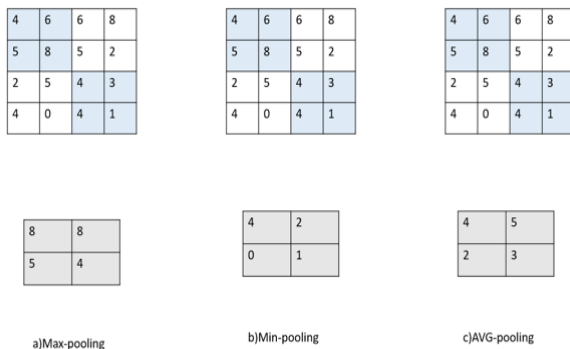


Fig. 5. Pooling Layer Results

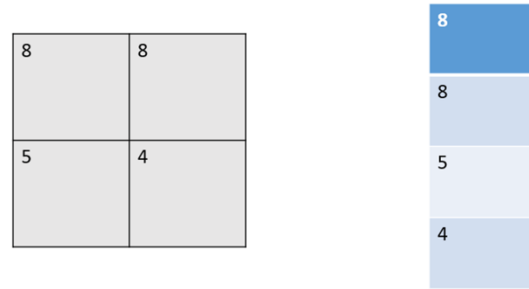


Fig. 6. Flattening Process

C. CNN Architectures

The significant improvement in CNN performance was mainly attributable to the restructuring of processing units and the development of new blocks. Utilizing the depth network to perform the novelist breakthroughs in CNN designs. The architecture of a model is a critical aspect when it comes to increasing the performance of many applications on various architectures such as ResNet and VGG [37].

- **Res Net** is divided into four stages: the network inputs the images with height and width multiples of 32 and a channel width of 3. The input size is assumed to be 224x224x3. For initial convolution and max-pooling, every ResNet50 design uses 7x7 and 3x3 kernel sizes. After that, the first stage starts with three residual blocks, each containing three layers. The kernels utilized to conduct the convolution operation in all three layers of the first stage block are 64, 64, and 28.
- **VGG:** during the training process, an RGB fixed-size image 224x224 was input into the VGG16 model ConvNets to preprocess each pixel by subtracting the average RGB value computed on the training set. The image is sent through a stack of convolutional layers. The receiving field is a 3x3 filter. The VGG16 model utilizes 1x1 convolutional filters in one setup. Spatial grouping is accomplished using five levels of grouping to follow some of the layer transformations. In the second step, the max-pooling is performed using a 2x2 pixel window. There is a SegNet design (a CNN architecture for semantic pixel-wise segmentation) for segmentation and an architecture consisting of an encoder network and a broad global semantic hashing structure, followed by a decoder network. The encoder in this experiment depends on the VGG16 classification network, followed by a decoder for this network. SegNet consists of a network encoder and a network decoder, followed by a pixel-wise classification layer. The cypher network contains 13 convolutional layers, which correspond to the 13 primary convolutional layers of the VGG16 network for the classification process. The decoder network has 13 layers because each encoder layer has a corresponding decoder layer. The final decoder output is sent to a multi-class SoftMax classifier, which individually generates class probabilities for each pixel [38].

IV. PROPOSED METHODOLOGY

The proposed method is a stage in which the severity of the disease is determined through three steps: 1) classifying COVID-19 and non-infected patients, 2) detecting the severity of the disease, and 3) carrying out the regression process that predicts the severity of the disease.

A. Classification Process for Detecting the COVID-19 Patients

Classification is a process related to categorization, where ideas and things are recognized, distinguished, and understood. In this methodology, the primary goal of CNN training is to classify image data based on features and find the convenient feature. ResNet50 training network is used in this work. To classify the lung image as infected or non-infected, ResNet50 models are trained on the optimized images obtained from the previous stage and used to classify any image after the preprocessing process to improve the tomography and use it in the training process.

In the proposed model, a neural network was trained to classify the image into two classes: COVID-19 or non-COVID-19. A large dataset of CT scan images, i.e., a publicly available COVID-19 CT scan dataset, was used to identify COVID-19; it contains 1252 CT scan images positive for COVID-19 and 1230 CT scan images negative for COVID-19, for a total of 2482 CT scan images. These data were collected from real patients in hospitals from São Paulo, Brazil, and data are available in [39].

The training process is performed to extract features based on specific criteria; if it is white in the lung image, this whiteness is often in the lower region of the lung based on medical studies and research. When the layer initially captures basic image features such as edges and blocks, they are considered as basic features grouped via the FC in each layer. These features are distributed into classes, which are determined in each layer. After each operation, the features are distributed to other classes in the second layer. Then, the convolution of these classes is grouped to determine which final class these belong to. The feature can be seen by visualizing the weight of the mesh filter from the first convolution layer, where the raw features are extracted after the first convolution layer.

After all the layers are processed, the last layer is processed in the ResNet50 product feature for all classes; this feature must be activated, and the training of the features maps must be saved, as they are labeled in the training for the classifier, to use this feature map in the training model to classify the output result. Finally, in this step, a multi-layer product is used to complete the training with an error-correction output model.

B. The Severity Detection Process

The process of determining the severity of the disease is carried out in three steps: 1) segmenting the inflammatory area, 2) segmenting the lung area, and 3) using the trained segmentation to determine the severity of the disease.

C. The Pneumonia-Segmentation Process

The classification process results are presented whether the patient has COVID-19 or not. In this step, the CT scan is used to detect the places representing pneumonia in the image by determining the percentage and extent of whiteness in the

lung. Image segmentation is one of the most complex phases of understanding the image content because of lighting, size, and orientation change. %% ref

Therefore, a fixed method of image-processing algorithms cannot be used, especially for medical images. To get around this problem, neural networks are used to train the computer to segment the image to handle image states dynamically. SegNet depends on VGG16, which is used for semantic segmentation. The pixel-classification layer is performed to predict the categorical label of each pixel in the input image. The dataset of COVID-19 CT scan images was used in this network, which contains 100 axial CT images from more than 40 patients with COVID-19, 70% training of the images, and 30% testing. Fig. 7 and Fig. 8 shows the flowchart that represents pneumonia and lung segmentation, respectively.

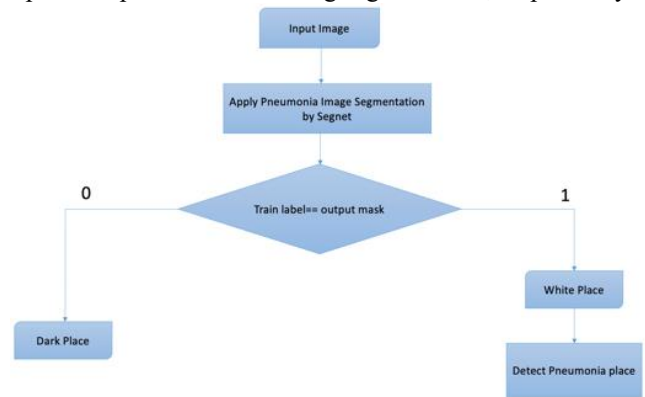


Fig. 7. Flowchart Representing Pneumonia Segmentation.

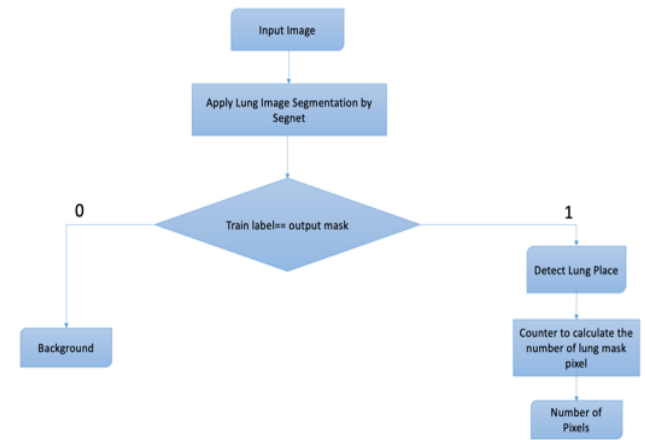


Fig. 8. Flowchart Representing Lung Segmentation.

The SegNet network defines the input and output images that indicate the segmentation mask images. The network is trained to find the output image through the database with mask images of inflammation for each image. These images are trained, such that the weight of the input image equals the weight of the output image. The last layer, which determines the category and provides the weight of the output image, is removed to train the images to reach the weight of the mask label by calculating the total pixels in white, the total pixels in black, and the ratio of the image to calculate the weight of the image.

Fig. 9, Fig. 10, and Fig. 11 show the result after applying the hash training model. Moreover, the training model recreates intrapulmonary pneumonia as shown in the hash-mask form. It also detects the lung boundaries as pneumonitis, meaning that there are regions incorrectly identified as areas with pneumonitis. Therefore, the lung area needs to be discovered.



Fig. 9. The Original Image



Fig. 10. Segmentation Mask

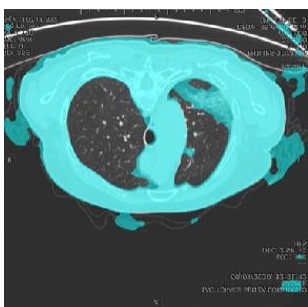


Fig. 11. Overlay Mask.

#### D. Lung-Segmentation Process

The severity of COVID-19 in the lung is determined to identify the edges of the lung. VGG16 has a high level of self-learning, adaptability, and generalization ability, with high training speed and accuracy of lung image recognition. Another semantic segmentation network was implemented using SegNet on VGG16. This kind of network needs to define the input and output image, which refer to the hash mask image that represents the lung places in the image. The network is trained to produce the output image through the database where there are mask images for each image are trained. These images label the mask by counting the total number of pixels in white and the number of pixels in black and their proportion to the image to calculate the weight of the image. This value will be within the weight of the resulting image, and it will be a mask image of inflammation. The training data are applied to the same images in the inflammation segmentation but with different segmentation-mask image files so that when the lung is located and the network is saved, then the lung and inflammation training

network are called and saved in the previous step to calculate and classify the lung opacity to discover the lung information in the images.

#### E. Using Segmentation Steps to Detect the Disease Severity

The VGG16 network is a Keras-based trained network. Keras is a neural network library that has been trained. These libraries make it simple to train images and preserve the networks that have been learned. ImageNet was used to train it on millions of images from a range of classifications [40]. Although training a CNN model from scratch takes longer than training a pre-trained model, it is less computationally costly when the dataset comprises fewer images. To categorize these characteristics, the fully connected neural network rule is employed, and the final layer is modified to provide it with a weighted representation of the output in the [0,1] range, where 1 denotes pneumonia and 0 represents the mask. After using the output of the lung image segmentation, the training network, and the output of the inflammation image segmentation both contain image information and main features. Then, it will be simple to obtain the location of inflammation in the lung using a set of computational steps and the area. As shown in Fig. 12, this model was applied to the same lung image to obtain a lung mask, and then the result of the lung mask was subtracted from the pneumonia mask until the areas that do not need it were reached. All-white areas outside the lung area were obtained, which represent bones and other areas that are not of interest. Exclusive OR (XOR), which is a logical process, was applied, such that when calculating the XOR between the image of the product of the subtraction process and with the pneumonia mask, the result will be lung inflammation location in the important area.

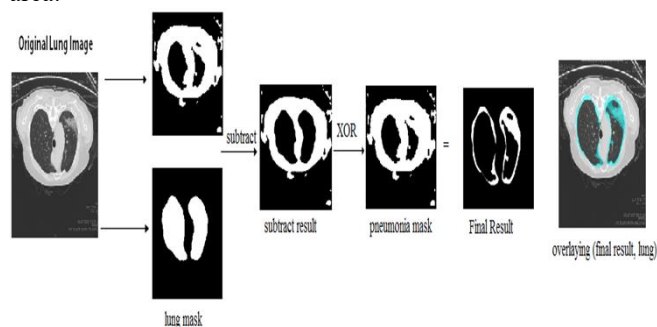


Fig. 12. The Detection of Pneumonia in lungs

Then, this result is applied to the original image to understand the location of the inflammation on the image. To calculate the severity, these steps are applied to all images and stored in a database containing the image number and disease percentage as represented in Table I, which represents a sample of the data, to prepare these data for the testing stage. These data are trained on CNN algorithms, and linear regression is applied to train the model to predict disease severity.

**Table I: Regression Dataset Sample**

Image No.	Training Data No.
Covid (1000).png	0.878708
Covid (1001).png	0.83667
Covid (1002).png	0.890259
Covid (1003).png	0.926618
Covid (1004).png	0.915866

### F. Regression Process

Regression analysis is a set of statistical methods used to estimate the relationships between a dependent variable and one or more variables in statistical modeling [41]. In this work, linear regression was used for analysis because the relationship between images and the proportion of inflammation is direct. At this stage, the dataset was collected and entered the model to discover the disease, determine the inflammation in the lung, and calculate the severity of the disease for each image. These images were stored with the percentage of each of them in the database, as represented in Fig. 13, which shows the number of images with the extent of the severity of the disease; this is used later in the training and testing process.

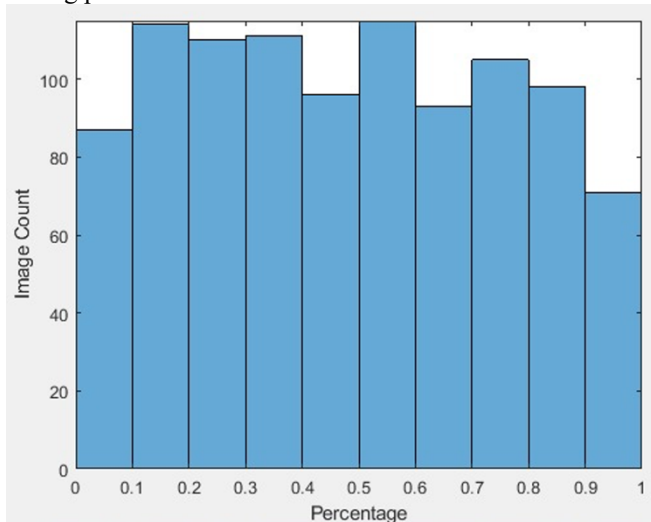


**Fig. 13. The Number of Images with the Extent of the Severity of the Disease.**

Before the training process is started, each one of the images is converted into values to be read in the process of regression analysis and converted into a 4D array, as shown in Fig. 14, because the regression analysis deals with values that do not deal with images.

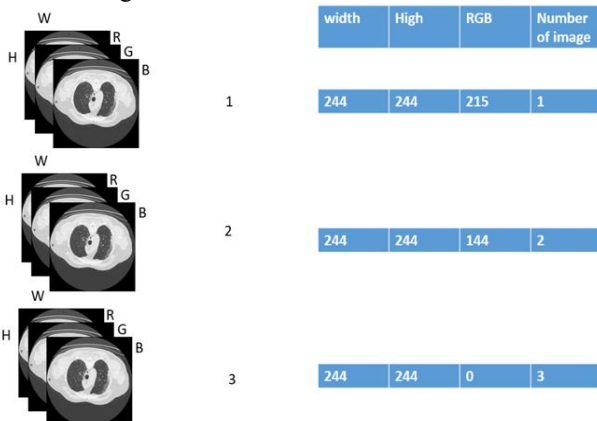


**Fig. 14. Converting an Image to a 4D Array.**

These data are applied to a CNN algorithm that built nine layers of a CNN that takes a range of real numbers and returns the output value from 0 to 1. The hidden layers in the CNN architecture contain four convolutional filters on the convolutional layer. The next layer is the maximum pool with sub-sampling ratios of 2x2. Fig. 15 represents a CNN model. The output layer is converted into a regression layer to train the network to predict the severity of the disease.

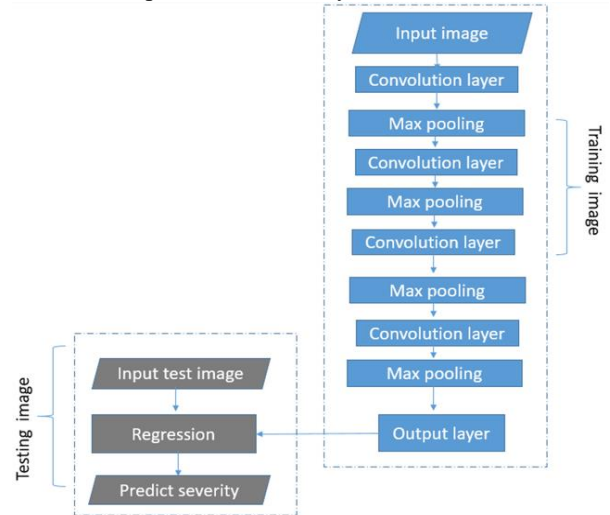


**Fig. 15. The CNN Model for the Regression Step.**

The method consists of two main parts of implementation and data operations. First, the training phase is where the images are input into the ResNet50 network to identify COVID-19 patients in order to transfer the learning to the segmentation phase, where the images are segmented. Both inflammation and lungs were analyzed on the VGG16 network to determine the location of inflammation in the lung. Second, the testing phase compiles these images with the severity of each image in the database to train these data to predict disease severity using linear regression. The CNN model works to predict and find the relationship between independent and dependent values. Each image is compared with its disease-severity rate. A value is expected for each image, and the equation is applied to find the error ratio between the true value and the expected values predicted by the algorithm. This relationship is represented between the variables shown in Fig. 16.

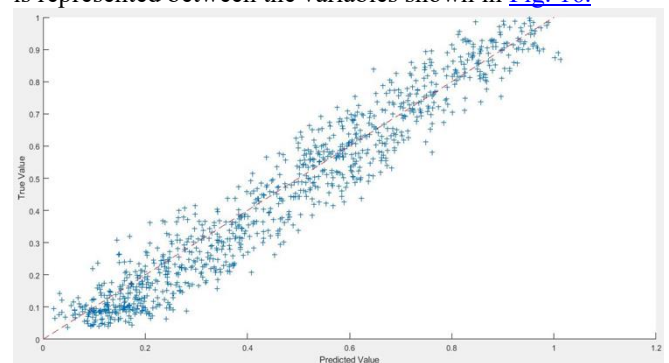


**Fig. 16. The Relationship between the Predicted Value and the True Value.**



In the first step, a matrix is constructed that contains the input images as input in the hash generator to create a database of images with a satisfactory severity percentage. In the regression stage, the difference between the true and expected values is taken, and the Root Mean Square Error Equation (RMSE) is applied. RMSE has been used as a standard statistical metric to measure model performance in meteorology. In this step, the threshold value is 0.15; it is chosen randomly based on previous experiments. It is necessary to determine this value because the result is based on the threshold value, which is the percentage of error from calculating the difference between the percentage of the actual image severity in the database and the expected percentage of disease severity for the test images.

### V. RESULTS

CNN relies on its ability to detect important features automatically without any human intervention. Data were trained on the ResNet50 network to classify patients with COVID-19 using CT images. The presence of pneumonia in the image is carried out by classifying the inflammation as the white areas of the lung, which are filled with fluid that leads to pneumonia. The images of COVID-19 patients were trained to determine disease severity using SegNet based on the VGG16 network and a 13-layer deep CNN. The value of the last layer was changed, with a label of 0 or 1. A database of 170 images was used to locate the lungs to quantify pneumonia using a segmentation mask for accurate comparison. The percentage of lung inflammation was measured by calculating the area of inflammation in the lung relative to the lung area, which gives the percentage of the volume of inflammation. Then, the severity of the disease was calculated for all the images collected in the database. Each image with the percentage severity of the disease was used in the linear regression process to predict the percentage severity of the disease.

#### A. Dataset

The dataset used in this work is defined as follows.

- The data were completed as truncated images containing positive images for 1252 COVID-19 images with COVID-19 infection and 1230 CT images without COVID-19 infection, for a total of 2482 CT images, to transfer the learning to the segmentation process, i.e., Kaggle [39].
- In the segmentation process, a dataset of 100 axial CT images of more than 40 patients infected with COVID-19 was taken and converted from JPG files. For the segmentation process of inflammation and disease from the radio, the data contain the segmentation mask for both lungs and the inflammation used in the training process. Fig. 17 and Fig. 18 show a sample of data images and samples of image masks for lungs, respectively. Fig. 19 shows the overlying image mask on the image used to obtain the lung location and its boundaries.

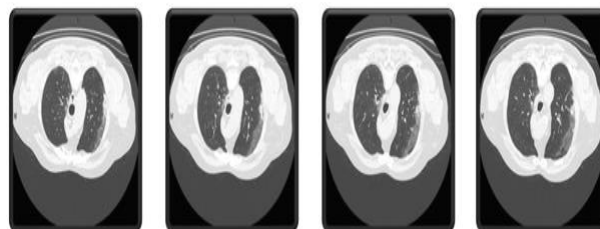


Fig. 17. Sample of Image Data.

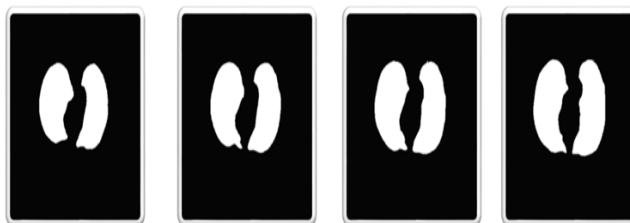


Fig. 18. An Image Mask of Lungs.

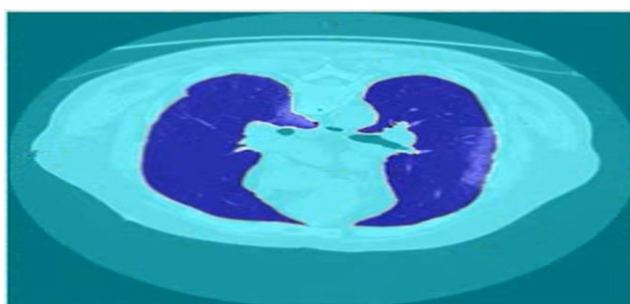


Fig. 19. Overlying Mask on Original Image.

MATLAB libraries were utilized to implement the research method, starting with preprocessing the data, followed by filtering and feature extraction, and finishing with classifications.

#### B. Testing and Training

The training, validating, and testing of the data were performed in this work. The sizes into which the data were split were 80% and 20%, 70% and 30%, and 50% and 50% for the training and for the testing, respectively. During the training phase, the data were split and shuffled to obtain the best accuracy. In the testing phase, the model was tested for all possible data and cases in dataset. The results from the training and testing phases are shown in Table II.

Table II: The Modeling Results of the Splitting Data

Phase	Dataset Size	Step 1	Step 2	Step 3
Classification process	2458	95.9%	95.7%	94.9%
Lung-segmentation process	174	98.72%	98.6%	98.1%
Pneumonia-segmentation process	174	96.5%	96.2%	95.5%
Regression process	1252	98.6%	98.29%	98%

Using several confusion-matrix-based performance matrices, the proposed DL-based COVID-19 classification model was tested using the following metrics: precision, recall, specificity, sensitivity, and accuracy.

C. Cross-Validation Accuracy

Cross-validation is a technique used to evaluate the individual model's performance of a data sample concerning future data by dividing the data into two groups: the training set, comprising the data where the application is carried out, and the testing set, comprising the data where the percentage of the resulting error is calculated. Cross-validation is usually used in statistics to perform the regression of a dataset, choose the best model to solve a particular problem and use it in classification. Five features were applied for validation, as represented in Table III, for the four phases used: classification, lung and pneumonia, and regression.

Table III: 5-fold Cross Validation Results

Phase	k= 1	k= 2	k= 3	k= 4	k= 5
Classification	95.3%	94.8%	94.6%	95.55%	96.2%
lung	98.5%	97.8%	98.5%	98.3%	98.9%
Pneumonia	94%	95.7%	96.1%	95.9%	95.9%
Regression	98.0%	97.5%	98.2%	98.35%	98.9%

D. Detection Results

The work is divided into (1) the classification of COVID-19 patients using ResNet50, (2) the image segmentation of COVID-19 patients, (3) the detection of the severity of disease in the lung, and (4) the prediction process based on the linear regression algorithm to predict the severity of the patients' disease.

E. Classification of COVID-19 Patients Using ResNet5

This study used DL to classify COVID-19 cases using a CNN model based on the ResNet50 architecture. To do so, 1253 images of COVID-19 patients and 1230 images of non-patients were used. We chose the ResNet50 network because it is one of the most widely used networks for classification, with an accuracy of 95.3% in training the data, as shown in Fig. 20.

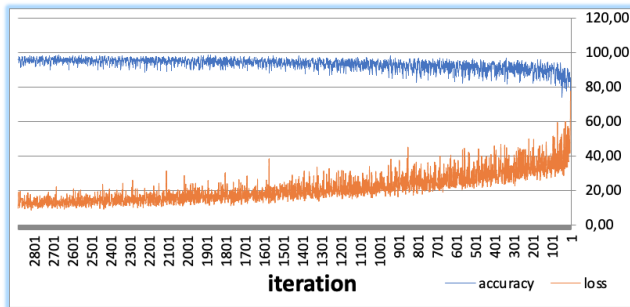


Fig. 20. The Training Accuracy of the Classification Process in ResNet50.

This step aims to determine whether the human is infected with COVID-19 or not. The confusion matrix shows that the model obtained the following values: a false negative of 0.0425, a true negative of 0.954, a true positive of 0.957, and a false positive of 0.045. Depending on the number of correct and incorrect predictions, the classifier performs well. The following performance measures are used to validate the proposed model's performance for the classification process, as shown in Table IV. The proposed framework yielded a high performance in the classification process. These values proved the reliability of the proposed framework in determining whether the given CT scan represented COVID-19 or not. The dataset was performed with 15 epochs using the ResNet50 method with a batch size of 24.

Table IV: The Classification Process Performance

Metric	Value
Accuracy	95.7%
Sensitivity	96.0%
Specificity	95.69%
Recall	95.7%
Precision	96.0%

F. Image Segmentation of COVID-19 Patients

There were significant differences between patients' CT scans, so the CNN can identify these differences. The images are segmented into two phases: inflammation (pneumonia) area segmentation, and lung area segmentation using SegNet based on the VGG16 network.

G. Segmentation of the Pneumonia Area

To identify the location of the inflammation and compare the input image to the output image of the segmentation mask, several experiments were performed on randomly selected images from the entire dataset to choose the most appropriate parameters to obtain the best segmentation performance. The dataset was divided into two parts, training datasets, 0.7, and testing datasets, 0.3. The total number of samples was 170, with an image size of 340x340. The training accuracy was 95.8%, as shown in Fig. 21, which shows the training accuracy and training loss; the model gives a high value to training accuracy. Moreover, it yields the best results in training with a high degree of flexibility because it approaches all points with the lowest validation and training loss.

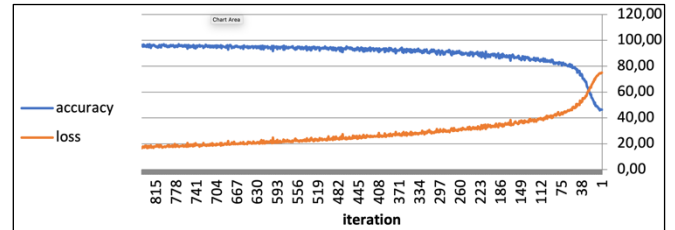


Fig. 21. Results of the Segmentation Process for Pneumonia Areas.

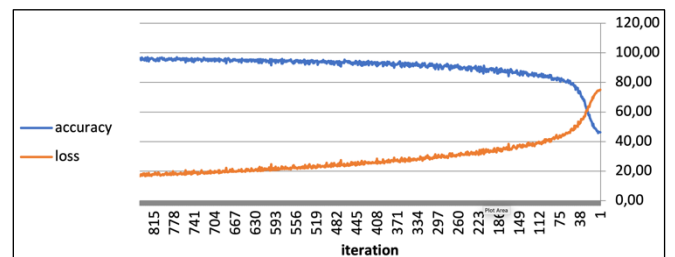


Fig. 22. Results of the Segmentation Process for both Lung Areas.

This step aims to segment the image into two parts by classifying them into labels, where 1 stands for inflammation (white regions) and 0 stands for non-inflammation regions. The training dataset was used up to a maximum of 100 Epochs using SegNet with a batch size of 3. The Performance of pneumonia- and lung- segmentation process are shown in Table V and Table VI, respectively.

**Table V: Pneumonia Segmentation Process Results**

Metric	Value
Accuracy	96.2%
Sensitivity	96.3%
Specificity	96.1%
Recall	96.27%
Precision	96.27%

**Table VI: Lung Segmentation Process Results**

Metric	Value
Accuracy	98.6%
Sensitivity	98.65%
Specificity	98.6%
Recall	98.6%
Precision	98.58%

**H. Segmentation of the Lung Area**

In order to determine the location of the lung using segmentation mask image, several experiments were performed on randomly selected images. The dataset was divided into two parts: training data sets with 0.7 and validation with 0.3. In the same sample, 170 images were used with an image size of 340x340. The training results are shown in Fig. 22, where the accuracy is 98.3%. To evaluate the performance, the training dataset was performed up to a maximum of 100 epochs using the SegNet with a batch size of 3. Results are shown in Table VI.

**I. Detection of Disease Severity**

One of the calculated results is the percentage of pneumonia, where sufficient information is available regarding lung and pneumonia areas and determining the state of the disease and the severity of the inflammation. As shown in Fig. 23, the percentage was calculated in several pathological conditions by subtracting the lung segmentation mask images from the segmented inflammation mask images. Furthermore, the XOR process was performed between the resulting image from the subtraction process and the image of the pneumonia mask to obtain the critical area, which is the area of pneumonia in the lung.

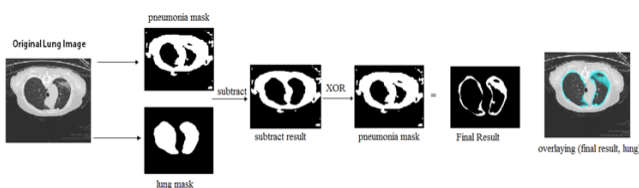


**Fig. 23. Detection of Disease Severity in Lungs**

By applying the classification to distinguish the image as COVID-19 or not, the segmentation operations were then applied to extract the inflammation area using the trained lung mask extraction network and the inflammation mask-extraction network. Then, by subtracting the lung mask from the inflammation mask, applying the XOR process on the image resulting from the subtraction process with the inflammation mask to obtain the inflammation area in the lung, and then dividing the number of pixels for each of the inflammation areas in the lung by the number of pixels in the lung, the percentage of inflammation is obtained for the image size. Fig. 24 shows the disease severity ratio of 0.1439.



**Fig. 24. The Percentage of Severity of Disease Value 0.1439**

Furthermore, the other cases that represent different severity levels of different images are shown in Figure. 17 The same method was applied to determine the severity. The more inflammation there is in the lung area, the greater the severity of the disease, as shown in the sixth case, in Fig. 25.

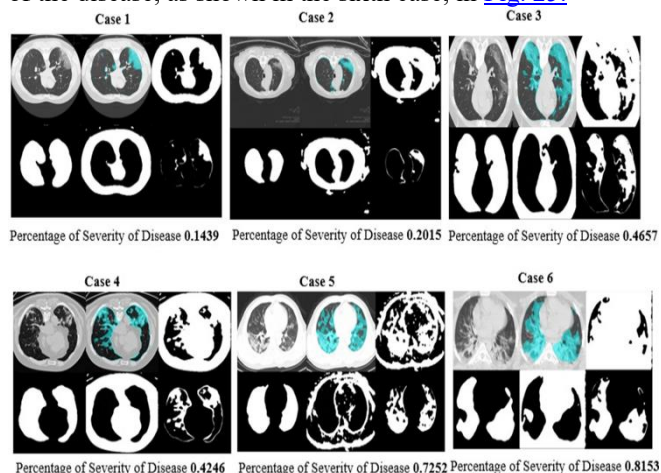


**Fig. 25. Different Cases for the Detection of Severity**

**J. Regression Analysis Process**

After the image dataset is created, it is compared with the dataset to predict the severity of the disease. For the prediction phase, any input images can be used to compare the input images with the database. In this step, the threshold value was 0.15, and it is necessary to be decided because the result is based on the threshold value. The prediction is performed by calculating the difference between the image in the database and the new images. The percentage of the prediction error is calculated through the difference between the actual values and the expected values. The RMSE is also calculated, which is the square root of the arithmetic mean of the sum of the square of the error rate. The threshold value is 0.15 and is used to calculate the number of images that match the expected ratio, and it is close to the true ratio, with a margin of error that is found by dividing by the sum of the true images to find the training RMSE. The training reached an RMSE of 0.07 and an accuracy of 98.29%.

## VI. COMPARISON WITH PREVIOUS STUDIES

Table VII shows that the proposed model achieved the highest accuracy in the four different processes using CT images of COVID-19 patients. All these studies used CT scan images.

**Table VII: Comparison of the Proposed Model with Previous Studies**

Ref.	Data Size	Dataset	Algorithm	Accuracy
[42]	2458	classification	ResNet50	95.7%
[43]	170	segmentation	CNN	98.6%
[44]	408	Regression	CNN	85.9%, RMSE = 0.49
The proposed model	2458	classification	ResNet50	95.7%
The proposed model	1252	regression	CNN	98.29%, RMSE = 0.07

The ResNet50 model in the classification process gave better results on CT images due to the improvements applied in the images, in which the important parts were improved. After several training stages, the preprocessing of the images played a key role in influencing the model, which led to the clarification of the features of the image. Moreover, the segmentation model gave a higher accuracy rate with the same database used in the segmentation process. The image segmentation mask plays a key role in determining the region's accuracy. The proposed model was based on lung segmentation based on the segmentation mask; this was achieved training the data to reach the weight of the mask image so that the image was accurately segmented based on the output image. Moreover, the regression model gave a higher accuracy rate with the same CNN approach used in other research and image regression training, which yielded a better result for RMSE based on the database generated from the process of determining disease severity than the proposed model.

## VII. CONCLUSION

This work proposed a systematic approach to COVID-19 detection, lung and lesion segmentation, and patients' course grading from the CT images. The proposed approach with the cascaded models achieved high performance levels in the segmentation and classification processes. The proposed approach with the ResNet50 model achieved the highest accuracy at 96.1% in terms of COVID-19-detection performance. The proposed model can classify COVID-19 patients. For lung segmentation, SegNet is performed to conduct feature extraction. The proposed pneumonia-segmentation pipeline can generate better lung and lesion masks for small lung areas. This study demonstrated lung segmentation using VGG16 and achieved the highest accuracy of 98.3% for lung and 95.8% for pneumonia. In summary, the system was able to classify the severity of COVID-19 in patients; computer-aided detection and quantification is an accurate, easy, and feasible method with which to diagnose COVID-19 cases. For future work, the proposed framework can be extended to solve more complex diagnostic problems, such as diagnosing the disease based on the doctors' diagnosis of critical and normal cases, analyzing these opinions based on each disease case, and finding the common factor of chronic diseases and their relationship with the affected person's impact on the disease. In addition, the

aim is to develop a different methodology using different data, such as the pathological record with the percentage of inflammation and the relationship between the pathological record and the extent of the disease's impact on the body.

## DECLARATION STATEMENT

Authors are required to include a declaration of accountability in the article, counting review-type articles, that stipulates the involvement of each author. The level of detail differs; Some subjects yield articles that consist of isolated efforts that are easily voiced in detail, while other areas function as group efforts at all stages. It should be after the conclusion and before the references.

Funding/ Grants/ Financial Support	No, I did not receive.
Conflicts of Interest/ Competing Interests	No conflicts of interest to the best of our knowledge.
Ethical Approval and Consent to Participate	No, the article does not require ethical approval and consent to participate with evidence.
Availability of Data and Material/ Data Access Statement	Not relevant.
Authors Contributions	The idea of the work was conceptualized by Mohammad Abbadi and Rania Alhalaseh. Methodology and validation were provided by Rania ALhalaseh. Software implementation and visualization were performed by Sura Kassasbeh. Writing---original-draft preparation was performed by Sura Kassasbeh, and writing---review and editing were performed by Rania Alhalaseh and Mohammad Abbadi. Project administration was performed by Mohammad Abbadi.

## REFERENCES

- Meters, W. *World Meters – Coronavirus*. [Online]. Available: <https://www.worldometers.info/coronavirus/>. [Accessed: June 2023].
- Organization, W.W.H. WHO Coronavirus (COVID-19) Dashboard. [Online]. Available: <https://covid19.who.int>. [Accessed: June 2023].
- Carfi, A.; Bernabei, R.; Landi, F.; et al. "Persistent symptoms in patients after acute COVID-19". *Jama* 2020, 324, 603–605. <https://doi.org/10.1001/jama.2020.12603>
- Ai, T.; Yang, Z.; Hou, H.; Zhan, C.; Chen, C.; Lv, W.; Tao, Q.; Sun, Z.; Xia, L. "Correlation of chest CT and RT-PCR testing for coronavirus disease 2019 (COVID-19) in China: a report of 1014 cases". *Radiology* 2020, 296, E32–E40. <https://doi.org/10.1148/radiol.2020200642>
- Li, W.T.; Ma, J.; Shende, N.; Castaneda, G.; Chakladar, J.; Tsai, J.C.; Apostol, L.; Honda, C.O.; Xu, J.; Wong, L.M.; et al. "Using machine learning of clinical data to diagnose COVID-19: a systematic review and meta-analysis". *BMC medical informatics and decision making* 2020, 20, 1–13. <https://doi.org/10.1186/s12911-020-01266-z>

6. Ghoshal, B.; Tucker, "A. Estimating uncertainty and interpretability in deep learning for coronavirus (COVID-19) detection". arXiv preprint arXiv:2003.10769 2020.
7. Maghddid, H.S.; Asaad, A.T.; Ghafoor, K.Z.; Sadiq, A.S.; Mirjalili, S.; Khan, M.K. "Diagnosing COVID-19 pneumonia from X-ray and CT images using deep learning and transfer learning algorithms". In Proceedings of the Multimodal image exploitation and learning 2021. SPIE, 2021, Vol. 11734, pp. 99–110. <https://doi.org/10.1117/12.2588672>
8. Sarker, I.H. "Deep Learning: A Comprehensive Overview on Techniques, Taxonomy, Applications and Research Directions". SN Computer Science; 2. Epub ahead of print 2021, 2021. <https://doi.org/10.1007/s42979-021-00815-1>
9. Liu, X.; Guo, S.; Yang, B.; Ma, S.; Zhang, H.; Li, J.; Sun, C.; Jin, L.; Li, X.; Yang, Q.; et al. "Automatic organ segmentation for CT scans based on super-pixel and convolutional neural networks". Journal of digital imaging 2018, 31, 748–760. <https://doi.org/10.1007/s10278-018-0052-4>
10. Ahmad, A.; Garhwal, S.; Ray, S.K.; Kumar, G.; Malebary, S.J.; Barukab, O.M. "The number of confirmed cases of covid-19 by using machine learning: Methods and challenges". Archives of Computational Methods in Engineering 2021, 28, 2645–2653. <https://doi.org/10.1007/s11831-020-09472-8>
11. Zoabi, Y.; Shomron, N. "COVID-19 diagnosis prediction by symptoms of tested individuals: a machine learning approach". MedRxiv 2020, pp. 2020–05. <https://doi.org/10.1101/2020.05.07.20093948>
12. Peng, M.; Yang, J.; Shi, Q.; Ying, L.; Zhu, H.; Zhu, G.; Ding, X.; He, Z.; Qin, J.; Wang, J.; et al. "Artificial Intelligence Application in COVID-19 Diagnosis and Prediction". COVID-19 Global literature on coronavirus disease - World Health Organization 2020. <https://doi.org/10.2139/ssrn.3541119>
13. Parekh, M.; Donuru, A.; Balasubramanya, R.; Kapur, S. "Review of the chest CT differential diagnosis of ground-glass opacities in the COVID era". Radiology 2020, 297, E289–E302. <https://doi.org/10.1148/radiol.2020202504>
14. Ozturk, T.; Talo, M.; Yildirim, E.A.; Baloglu, U.B.; Yildirim, O.; Acharya, U.R. "Automated detection of COVID-19 cases using deep neural networks with X-ray images". Computers in biology and medicine 2020, 121, 103792. <https://doi.org/10.1016/j.combiomed.2020.103792>
15. Alazab, M.; Venkatraman, S.; Watters, P.; Alazab, M. "Information security governance: the art of detecting hidden malware". In IT security governance innovations: theory and research; IGI Global, 2013; pp. 293–315. <https://doi.org/10.4018/978-1-4666-2083-4.ch011>
16. LeCun, Y.; Bengio, Y.; Hinton, G. "Deep learning". nature 2015, 521, 436–444. <https://doi.org/10.1038/nature14539>
17. Naudé, W. "Artificial Intelligence against COVID-19: An early review" 2020. IZA Discussion Papers, No. 13110, Institute of Labor Economics (IZA), Bonn. [Online] Available: [ <https://www.econstor.eu/handle/10419/216422>]. [August: June 2023]. <https://doi.org/10.2139/ssrn.3568314>
18. Pouyanfar, S.; Sadiq, S.; Yan, Y.; Tian, H.; Tao, Y.; Reyes, M.P.; Shyu, M.L.; Chen, S.C.; Iyengar, S.S. "A survey on deep learning: Algorithms, techniques, and applications". ACM Computing Surveys (CSUR) 2018, 51, 1–36. <https://doi.org/10.1145/3234150>
19. Narin, A.; Kaya, C.; Pamuk, Z. "Automatic detection of coronavirus disease (covid-19) using x-ray images and deep convolutional neural networks". Pattern Analysis and Applications 2021, 24, 1207–1220. <https://doi.org/10.1007/s10044-021-00984-y>
20. Srivastava, N.; Hinton, G.; Krizhevsky, A.; Sutskever, I.; Salakhutdinov, R. "Dropout: a simple way to prevent neural networks from overfitting". The journal of machine learning research 2014, 15, 1929–1958.
21. Mahdy, L.N.; Ezzat, K.A.; Elmousalimi, H.H.; Ella, H.A.; Hassaniien, A.E. "Automatic X-ray COVID-19 Lung Image Classification 664System based on Multi-Level Thresholding and Support Vector Machine". MedRxiv 2020, pp. 2020–03. <https://doi.org/10.1101/2020.03.30.20047787>
22. Alzubaidi, L.; Zhang, J.; Humaidi, A.J.; Al-Dujaili, A.; Duan, Y.; Al-Shamma, O.; Santamaria, J.; Fadhel, M.A.; Al-Amidie, M.; Farhan, L. "Review of deep learning: Concepts, CNN architectures, challenges, applications, future directions". Journal of big Data 2021, 8, 1–74. <https://doi.org/10.1186/s40537-021-00444-8>
23. Rajakumar, G.; Leela, R.S.J.; Darney, P.E.; Narayanan, K.L.; Krishnan, R.S.; Robinson, Y.H. "Seg-Net: Automatic Lung Infection Segmentation of COVID-19 from CT images". In Proceedings of the 2021 5th International Conference on Trends in Electronics and Informatics (ICOEI). IEEE, 2021, pp. 739–744. <https://doi.org/10.1109/ICOEI51242.2021.9453022>
24. Simonyan, K.; Zisserman, A. "Very Deep Convolutional Networks for Large-Scale Image Recognition". arXiv 1409.1556 2014.
25. Zhu, J.S.; Ge, P.; Jiang, C.; Zhang, Y.; Li, X.; Zhao, Z.; Zhang, L.; Duong, T.Q. "Deep-learning artificial intelligence analysis of clinical variables predicts mortality in COVID-19 patients". Journal of the American College of Emergency Physicians Open 2020, 1, 1364–1373. <https://doi.org/10.1002/emp2.12205>
26. Sharma, S. "Drawing insights from COVID-19 -infected patients using CT scan images and machine learning techniques: a study on 200 patients". Environmental Science and Pollution Research 2020, 27, 37155–37163. <https://doi.org/10.1007/s11356-020-10133-3>
27. Kundu S, Elhalawani H, Gichoya JW, Kahn CE Jr. "How Might AI and Chest Imaging Help Unravel COVID-19's Mysteries?". Radiol Artif Intell. 2020 May 6;2(3):e200053. doi: 10.1148/ryai.2020200053. PMID: 33928254; PMCID: PMC7233385. <https://doi.org/10.1148/ryai.2020200053>
28. Neri, E.; Miele, V.; Coppola, F.; Grassi, R. "Use of CT and artificial intelligence in suspected or COVID-19 positive patients: statement of the Italian Society of Medical and Interventional Radiology". La radiologia medica 2020, 125, 505–508. <https://doi.org/10.1007/s11547-020-01197-9>
29. Zhang, K.; Liu, X.; Shen, J.; Li, Z.; Sang, Y.; Wu, X.; Zha, Y.; Liang, W.; Wang, C.; Wang, K.; et al. "Clinically applicable AI system for accurate diagnosis, quantitative measurements, and prognosis of COVID-19 pneumonia using computed tomography". Cell 2020, 181, 1423–1433. <https://doi.org/10.1016/j.cell.2020.04.045>
30. Wang, S.; Zha, Y.; Li, W.; Wu, Q.; Li, X.; Niu, M.; Wang, M.; Qiu, X.; Li, H.; Yu, H.; et al. "A fully automatic deep learning system for COVID-19 diagnostic and prognostic analysis". European Respiratory Journal 2020, 56. <https://doi.org/10.1101/2020.03.24.20042317>
31. Oh, Y.; Park, S.; Ye, J.C. "Deep learning COVID-19 Features on CXR using Limited Training Data Sets". IEEE transactions on medical imaging 2020, 39, 2688–2700. <https://doi.org/10.1109/TMI.2020.2993291>
32. Wu, P.; Sun, X.; Zhao, Z.; Wang, H.; Pan, S.; Schuller, B. "Classification of lung nodules based on deep residual networks and migration learning". Computational intelligence and neuroscience 2020, 2020. <https://doi.org/10.1155/2020/8975078>
33. Wong, H.Y.F.; Lam, H.Y.S.; Fong, A.H.T.; Leung, S.T.; Chin, T.W.Y.; Lo, C.S.Y.; Lui, M.M.S.; Lee, J.C.Y.; Chiu, K.W.H.; Chung, T.W.H.; et al. "Frequency and distribution of chest radiographic findings in patients positive for COVID-19". Radiology 2020, 296, E72–E78. <https://doi.org/10.1148/radiol.2020201160>
34. Cohen, J.P.; Dao, L.; Roth, K.; Morrison, P.; Bengio, Y.; Abbasi, A.F.; Shen, B.; Mahsa, H.K.; Ghassemi, M.; Li, H.; et al. "Predicting covid-19 pneumonia severity on chest x-ray with deep learning". Cureus 2020, 12. <https://doi.org/10.7759/cureus.9448>
35. Zhu, J.S.; Ge, P.; Jiang, C.; Zhang, Y.; Li, X.; Zhao, Z.; Zhang, L.; Duong, T.Q. "Deep-learning artificial intelligence analysis of clinical variables predicts mortality in COVID-19 patients". Journal of the American College of Emergency Physicians Open 2020, 1, 1364–1373. <https://doi.org/10.1002/emp2.12205>
36. Kaur, M.; Kaur, J.; Kaur, J. "Survey of contrast enhancement techniques based on histogram equalization". International Journal of Advanced Computer Science and Applications 2011, 2. <https://doi.org/10.14569/IJACSA.2011.020721>
37. Yamashita, R.; Nishio, M.; Do, R.K.G.; Togashi, K. "Convolutional neural networks: an overview and application in radiology". Insights into imaging 2018, 9, 611–629. <https://doi.org/10.1007/s13244-018-0639-9>
38. Badrinarayanan, V.; Kendall, A.; Cipolla, R. "Segnet: A deep convolutional encoder-decoder architecture for image segmentation". IEEE transactions on pattern analysis and machine intelligence 2017, 39, 2481–2495. <https://doi.org/10.1109/TPAMI.2016.2644615>
39. Soares, E.; Angelov, P.; Biaso, S.; Froes, M.H.; Abe, D.K. "SARS-CoV-2 CT-scan dataset: A large dataset of real patients CT scans for SARS-CoV-2 identification". MedRxiv 2020, pp. 2020–04.
40. Hernandez-Sequeira, I.; Fernandez-Beltran, R.; Pla, F. "Transfer Deep Learning for Remote Sensing Datasets: A Comparison Study". In Proceedings of the IGARSS 2022-2022 IEEE International Geoscience and Remote Sensing Symposium. IEEE, 2022, pp. 3207–

3210. <https://doi.org/10.1109/IGARSS46834.2022.9884667>
41. Ng, S.F.; Chew, Y.M.; Chng, P.E.; Ng, K.S. "An insight of linear regression analysis. Scientific Research Journal 2018, 15, 1–16. <https://doi.org/10.24191/srj.v15i2.5477>
  42. Bharati, S.; Podder, P.; Mondal, M.R.H. "Hybrid deep learning for detecting lung diseases from X-ray images". Informatics in Medicine Unlocked 2020, 20, 100391. <https://doi.org/10.1016/j.imu.2020.100391>
  43. Liang, H.; Guo, Y.; Chen, X.; Ang, K.L.; He, Y.; Jiang, N.; Du, Q.; Zeng, Q.; Lu, L.; Gao, Z.; et al. "Artificial intelligence for stepwise diagnosis and monitoring of COVID-19". European radiology 2022, pp. 1–11. <https://doi.org/10.1007/s00330-021-08334-6>
  44. Zhu, X.; Song, B.; Shi, F.; Chen, Y.; Hu, R.; Gan, J.; Zhang, W.; Li, M.; Wang, L.; Gao, Y.; et al. "Joint prediction and time estimation of COVID-19 developing severe symptoms using chest CT scan". Medical image analysis 2021, 67, 101824. <https://doi.org/10.1016/j.media.2020.101824>

### AUTHORS PROFILE



**Rania Alhalaseh** is an assistant professor at data science department, faculty of Information Technology, Mutah University. She got her bachelor's degree in computer information system in 2004 and masters in computer science in 2006 from the university of Jordan. She got her Ph.D in computer science from TU Berlin. From 2006 until 2008 she worked as a lecturer at computer science department at Mutah University. She served as the head of data science department from 2021- 2023. Her research interest includes advanced machine learning and deep learning, applied artificial intelligence, biometrics, human computer interaction, discrete mathematics, database analysis, feature extraction, computer vision, graph analysis, computer algorithms, information extraction, image data analysis, and social network analysis. She has an IEEE Computer Society membership.



**Mohammad Abbadi** is a professor of Image Processing at Department of Computer Science, Faculty of Information Technology, Mutah University. He got his bachelor's degree in computer science from Mutah university, and master's degree from George Washington University. He got his Ph.D. in computer science from George Washington University in 2000. He served as the dean of Information Technology Faculty at Mutah from 2020 - 2023. His research interest includes multimedia, networks, blended and e-learning, data compression, machine and deep learning, image processing, discrete mathematics, computer algorithms, pattern recognition, computer vision, applied artificial intelligence, information extraction, image data analysis, and biometrics. He has an IEEE Computer Society membership.



**Sura Kassarbeh** has a master's degree in computer science from Mutah University, she graduated in 2021. She got her bachelor's degree in computer science from Mutah university in 2017. She is working as a researcher and teacher assistant in computer science department at Mutah university, she started in 2022. Her research interest includes machine and deep learning, image processing, computer vision, computer algorithms, database, and biometrics. Her master thesis was entitled: "Deep Learning Approach for Covid-19 Advanced Analysis".

**Disclaimer/Publisher's Note:** The statements, opinions and data contained in all publications are solely those of the individual author(s) and contributor(s) and not of the Blue Eyes Intelligence Engineering and Sciences Publication (BEIESP)/ journal and/or the editor(s). The Blue Eyes Intelligence Engineering and Sciences Publication (BEIESP) and/or the editor(s) disclaim responsibility for any injury to people or property resulting from any ideas, methods, instructions or products referred to in the content.